

Is there a concordance value for H_0 ?

Vladimir V. Luković¹, Rocco D'Agostino¹, and Nicola Vittorio^{1,2}

¹ Dipartimento di Fisica, Università di Roma "Tor Vergata", Via della Ricerca Scientifica 1, I-00133, Roma, Italy

² Sezione INFN, Università di Roma "Tor Vergata", Via della Ricerca Scientifica 1, I-00133, Roma, Italy

Received / Accepted

ABSTRACT

Context. We test the theoretical predictions from a number of cosmological models against different observables, to compare the indirect estimates of the present expansion rate, coming from model fitting, with the direct measurements based on Cepheids data from Riess et al. (2016).

Aims. We perform a statistical analysis of SN Ia, Hubble parameter and baryonic acoustic oscillation data. A joint analysis of these datasets allows to better constrain cosmological parameters, but also to break the degeneracy that appears in the distance modulus definition between H_0 and the absolute B-band magnitude of SN Ia, M_0 .

Methods. From the theoretical side, we consider flat and non-flat Λ CDM, w CDM, and inhomogeneous LTB models. For the analysis of SN Ia we follow the approach suggested by Trøst Nielsen et al. (2015) to take into account the distributions of SN Ia intrinsic parameters.

Results. For the Λ CDM model we find that $\Omega_m = 0.35 \pm 0.02$, $H_0 = (67.8 \pm 1.0) \text{ km s}^{-1}/\text{Mpc}$, while the corrected SN absolute magnitude has a Normal distribution $\mathcal{N}(19.13, 0.11)$. The w CDM model provides the same value for Ω_m , while $H_0 = (66.5 \pm 1.8) \text{ km s}^{-1}/\text{Mpc}$ and $w = -0.93 \pm 0.07$. When an inhomogeneous LTB model is considered, the combined fit provides $H_0 = (64.2 \pm 1.9) \text{ km s}^{-1}/\text{Mpc}$.

Conclusions. Both the Akaike Information Criterion and the Bayesian factor analysis cannot clearly distinguish between Λ CDM and w CDM cosmologies, while they clearly disfavour the LTB model. Concerning Λ CDM, our joint analysis of the SN Ia, the Hubble parameter and the baryonic acoustic oscillation datasets provides H_0 values that are consistent with CMB-only Planck measurements, but 1.7σ and 2.5σ away from the values presented by Efstathiou (2014) and Riess et al. (2016), respectively. Therefore, the need to go beyond the concordance Λ CDM model still remains an open question.

Key words. cosmology: cosmological parameters, distance scale, dark matter, dark energy

1. Introduction

Since the early Hubble's determination (Hubble 1929), the Hubble constant was for a long period believed to be between 50 and $100 \text{ km s}^{-1}/\text{Mpc}$ (Kirshner 2003). The recent findings are obtained by means of space facilities, improved control of systematics and the use of different calibration techniques, as in the Hubble Space Telescope Key Project, which estimated $H_0 = (72 \pm 8) \text{ km s}^{-1}/\text{Mpc}$ (Freedman et al. 2001). Riess et al. (2016) provide the most recent direct estimate of the expansion rate of the Universe: $H_0 = (73.0 \pm 1.8) \text{ km s}^{-1}/\text{Mpc}$. Together with this extraordinary improvements in the direct determination of the distance ladder, there are by now different classes of observations that allow an indirect estimate of the Hubble constant. Among others, the observations of the cosmic microwave background (CMB) anisotropy by WMAP (Hinshaw et al. 2013) and Planck Collaboration (2015) satellites yielded values of $H_0 = (70.0 \pm 2.2) \text{ km s}^{-1}/\text{Mpc}$ and $H_0 = (67.27 \pm 0.66) \text{ km s}^{-1}/\text{Mpc}$, respectively. Besides the CMB anisotropy measurements, other observables have been crucial to constrain the cosmological parameters, such as type Ia Supernovae (SN Ia). The High- z Supernova Search Team led by Adam Riess together with Brian P. Schmidt (Riess et al. 1998) and the Supernova Cosmology Project led by Saul Perlmutter (Perlmutter et al. 1999) gave the first evidence for an accelerated cosmic expansion. Since then, the number of observed SN Ia increased by about an order of magnitude. Different publicly available compilations have been used to constrain cosmological models: Union2 (Amanul-

lah et al. 2010), Union2.1 (Suzuki et al. 2012), Constitution set (Hicken et al. 2009), JLA (Betoule et al. 2014). The results confirm the need for a late accelerated expansion of the Universe, consistently with the findings of the WMAP and Planck missions. Unfortunately, the observations of SN Ia by themselves are not able to provide a value for the local expansion rate of the Universe, H_0 , since this parameter is degenerate with the SN absolute magnitude. However, there are other cosmological observables that are more directly sensitive to the value of the Hubble constant. From one hand, passively-evolving red galaxies, dominated by the older stellar population, whose age can be accurately estimated from a spectroscopic analysis (also known as cosmic chronometers), can be used to provide the redshift dependence of the expansion rate, $H(z)$, as suggested by Jimenez & Loeb (2002). Fitting these observational Hubble data (OHD), Liu et al. (2015) found a value of $H_0 = 67.6 \text{ km s}^{-1}/\text{Mpc}$. On the other hand, the baryon acoustic oscillation (BAO) data have been used to constrain the cosmological parameters, providing results in agreement with the most recent findings of the Planck Collaboration. In particular, a recent estimate of the Hubble constant provides $H_0 = (68.11 \pm 0.86) \text{ km s}^{-1}/\text{Mpc}$ (Cheng & Huang 2015).

It is clear that the indirect estimates of the Hubble constant lead to smaller values of H_0 compared to the direct measurements. In fact, both the earlier estimate of $H_0 = (73.8 \pm 2.4) \text{ km s}^{-1}/\text{Mpc}$ by Riess et al. (2011) and the latest one (Riess et al. 2016) are in tension with the most recent result from Planck (TT, TE, EE + lowP) at the 2.6σ and 3.0σ level, respectively. The question to be asked is whether this tension hides new physics beyond what is by now commonly called the con-

Send offprint requests to: vladimir.lukovic@roma2.infn.it

cordance model. This point has been addressed by Efstathiou (2014) who reanalysed the Riess et al. (2011) Cepheid data. They obtained a value $H_0 = (72.5 \pm 2.5) \text{ km s}^{-1}/\text{Mpc}$, reducing the tension with Planck to only 2σ and concluding that there is no evidence for new physics. In our work we want to extend this discussion to see if any tension is present when observables other than CMB are considered.

The quality of the SN Ia data suggests to perform a combined analysis with both the OHD and BAO data, to break the degeneracy between the SN absolute magnitude and the Hubble constant, peculiar to the SN analysis. A number of SN datasets (such as Union and Constitution) provide cosmological distance moduli that are derived *assuming* a flat Λ CDM model, hence these datasets should be cautiously treated in constraining cosmological models different from the concordance one. In our work, we use the JLA dataset that provides model-independent apparent magnitudes instead of model-dependent distance moduli. Moreover, the increase in the amount of data and the improvement in systematics imply the need for a more complete statistical analysis. This is why we follow the approach proposed by Trøst Nielsen et al. (2015) for the SN data analysis. As far as the theoretical models are concerned, we consider the standard flat Λ CDM model and its extensions that include: the curvature-free $k\Lambda$ CDM model; a dark energy model characterised by an equation of state (EoS) $p = w\rho c^2$, with $w = \text{const}$. In addition, we also consider a different class of models, based on the Lemaître-Tolman-Bondi (LTB) metric, which describes an isotropic but inhomogeneous Universe (Lemaître 1933; Tolman 1934; Bondi 1947; Krasiński 1997), to stress the dependence of the Hubble constant estimates on the assumed theoretical model.

The plan of the paper is as follows. In Section 2 we review the theoretical models we will be working with. In Section 3 we review the observables and datasets used in our analysis. In Section 4 we show the results of our comparison between theory and observations. Finally, in Section 6 we summarise our findings and conclusions.

2. Theoretical models

All the models considered here arise from the exact solutions of the Einstein field equations (EE) $G^\mu{}_\nu = \kappa T^\mu{}_\nu$, where $G^\mu{}_\nu$ is the Einstein tensor, $\kappa = 8\pi G/c^4$ and $T^\mu{}_\nu = \text{diag}(\rho c^2, -p, -p, -p)$ is the form of the energy-momentum tensor for a perfect fluid in the comoving frame. Here p and ρ – pressure and density of the fluid – are related by the equation of state (EoS) $p = w\rho c^2$.

2.1. FLRW models

Friedmann-Lemaître-Robertson-Walker (FLRW) models describe a homogeneous and isotropic Universe. Under such conditions, EE can be solved exactly resulting to the metric (Friedmann 1922, 1924; Robertson 1935; Walker 1937)

$$ds^2 = c^2 dt^2 - R^2(t) \left[\frac{dr^2}{1 - kr^2} + r^2(d\theta^2 + \sin^2\theta d\phi^2) \right] \quad (1)$$

where $R(t)$ is a scale factor in units of length and $k = -1, 0, +1$ is a curvature parameter for the open, flat and closed 3D space geometry, respectively. The Hubble expansion rate as a function of redshift is defined as

$$H(z) \equiv d(\ln R)/dt = -(1+z)^{-1} dz/dt \quad (2)$$

Using the Friedmann equation, it can be expressed as

$$H(z) = H_0 E(z) \quad (3)$$

where $H_0 \equiv H(z=0)$, while the adimensional Hubble parameter $E(z)$ is given by

$$E(z) = \sqrt{\sum_i \Omega_i (1+z)^{3(1+w_i)} + \Omega_k (1+z)^2} \quad (4)$$

Here $\Omega_k \equiv -kc^2/[H_0^2 R(t_0)^2]$ and t_0 is the age of the Universe, while the sum runs over all the components of the cosmological fluid – each characterised by its own EoS and density parameter, $\Omega_i \equiv \rho_i/\rho_c$, the present density of the i -th component in units of the critical density $\rho_c = 8\pi G/(3H_0^2)$. The functional dependence of the luminosity distance with the redshift is fixed by the cosmological model. In FLRW model $d_L(z)$ is calculated according to the equation

$$d_L(z) = \frac{c(1+z)}{H_0 \sqrt{|\Omega_k|}} S_k \left[\sqrt{|\Omega_k|} \int_0^z \frac{dz'}{E(z')} \right] \quad (5)$$

where the function S_k depends on the curvature:

$$S_k(\tau) \equiv \begin{cases} \sin \tau & \text{for } k = +1 \\ \tau & \text{for } k = 0 \\ \sinh \tau & \text{for } k = -1 \end{cases} \quad (6)$$

Eqs. (3) and (5) will be used in Section 4 to fit theoretical models to observables such as the Hubble expansion rate and the SN Ia.

There is an overwhelming evidence that about a quarter of the critical density in the Universe is in the form of a cold, weakly interacting dark matter (CDM) and that an extra component in the cosmological fluid is needed for closing the Universe. Although the physical nature of this dark energy (DE) component is poorly understood, it provides at the moment the only explanation for the accelerated expansion of the Universe in a FLRW cosmology (Riess et al. 1998; Perlmutter et al. 1999). In fact, the second Friedmann equation

$$\frac{\ddot{a}}{a} = -\frac{4\pi G}{3} \sum_i \rho_i (1 + 3w_i) \quad (7)$$

shows that for the cosmic fluid to be in an accelerated expansion at least one component must have $w < -1/3$. The density evolution is provided by the time component of the conservation equations $T^{\alpha\beta}{}_{;\beta} = 0$:

$$\frac{d\rho}{da} + \frac{3\rho}{a} (w + 1) = 0 \quad (8)$$

Whereas DM is more constrained and usually considered cold and pressureless ($w \equiv 0$), the DE models consider various EoS for DE fluid. For $w \equiv -1$, the dark energy density is constant (cf. Eq. (8)) and it can be described in terms of a non-vanishing cosmological constant $\Lambda = 8\pi G\rho_\Lambda/c^2$. This case recovers the flat concordance Λ CDM model considered to be the simplest way of best-fitting current cosmological observations. We will also consider the case of a w CDM model with $-1 < w < -1/3$, which we assume to be constant with respect to the cosmic expansion.

2.2. LTB models

In order to explain the accelerated expansion suggested by SN Ia observations, the homogeneous and isotropic FLRW model must resort to DE. However, the same effect can be explained in an alternative way, by relaxing the homogeneity requirement of the Cosmological Principle and presuming an isotropic Gpc-size underdensity in matter distribution (see e.g. Alnes et al. (2006)).

Under pressureless conditions, the local isotropic, but inhomogeneous Universe is described by the LTB metric

$$ds^2 = c^2 dt^2 - \frac{R'^2(r, t)}{1 - k(r)} dr^2 - R^2(r, t) [d\theta^2 + \sin^2 \theta d\phi^2] \quad (9)$$

where $k(r)$ determines the spatial curvature of 3D space. We denote derivatives with respect to the comoving radial coordinate r and to the time t with prime and overdot symbols, respectively. As before, $R(r, t)$ is the scale factor in units of length, and we can introduce the reduced scale factor as well: $a(r, t) \equiv R(r, t)/R_0(r)$, with $R_0(r) \equiv R(r, t_0)$. Unlike the standard model, in LTB models there exist two expansion rates, the radial and the transverse one:

$$H_{\parallel}(r, t) \equiv \frac{\dot{R}(r, t)}{R'(r, t)} \quad (10)$$

$$H_{\perp}(r, t) \equiv \frac{\dot{R}(r, t)}{R(r, t)} = \frac{\dot{a}(r, t)}{a(r, t)} \quad (11)$$

Obviously, at the centre of symmetry $H_{\parallel}(r = 0, t) \equiv H_{\perp}(r = 0, t)$. Then, the local expansion rate at the present time, t_0 , is given by

$$H_0 = H_{\parallel}(r = 0, t_0) = H_{\perp}(r = 0, t_0) \quad (12)$$

One should note that, as in the FLRW metric, r is an adimensional coordinate and it is not a measure of a physical distance. Being a flag coordinate, we have the freedom of rescaling r such that, for example, $R_0(r) = c t_0 \times r$. As we are considering an isotropic, but inhomogeneous fluid, all its parameters such as pressure, density and EoS parameter w may in principle depend not only on time, but also on the radial coordinate. For LTB models we consider the cosmic fluid with two components: the pressureless inhomogeneous cold matter (with $w \equiv 0$) and the dark energy fluid (with trivial EoS parameter $w \equiv -1$). Such a DE fluid component is equivalent to having an inhomogeneous Λ term that is constant in time and on every sphere of radius r , but with a possible radial profile $\Lambda(r)$. Recalling the Birkhoff theorem, we can expect that each shell evolves independently of the others, as a FLRW model with the same values of the fluid parameters. Hence, solving EE leads to the analogous of the Friedmann equation

$$H_{\perp}^2(r, t) = H_0^2(r) \left[\frac{\Omega_m(r)}{a(r, t)^3} + \frac{\Omega_k(r)}{a(r, t)^2} + \Omega_{\Lambda}(r) \right] \quad (13)$$

Here $H_0(r) \equiv H_{\perp}(r, t_0)$. As in the FLRW model, $\Omega_m(r) \equiv 8\pi G \rho_m(r)/3H_0^2(r)$, $\Omega_{\Lambda}(r) \equiv \Lambda(r)c^2/3H_0^2(r)$ and $\Omega_k(r) \equiv -k(r)c^2/[H_0^2(r)R_0^2(r)]$ are rescaled densities in units of the critical density. Note that still, for each shell, we have $\Omega_m(r) + \Omega_k(r) + \Omega_{\Lambda}(r) \equiv 1$. Eq. (13) is a differential equation for $a(r, t)$ [c.f. Eq. (11)]. In the most general case, it can be solved only numerically. Here we will concentrate our analysis on two special cases for which Eq. (13) can be solved analytically, namely $\Omega_{\Lambda}(r) \equiv 0$ and $\Omega_k(r) \equiv 0$. The solution of the former one is:

$$\left. \begin{aligned} a(r, t) &= \frac{\Omega_m(r)}{2\Omega_k(r)} (\cosh \eta - 1) \\ t - t_B(r) &= \frac{1}{2H_0(r)} \frac{\Omega_m(r)}{\Omega_k^{3/2}(r)} (\sinh \eta - \eta) \end{aligned} \right\} \Omega_k(r) > 0 \quad (14)$$

$$\left. \begin{aligned} a(r, t) &= \frac{\Omega_m(r)}{2|\Omega_k(r)|} (1 - \cos u) \\ t - t_B(r) &= \frac{1}{2H_0(r)} \frac{\Omega_m(r)}{|\Omega_k(r)|^{3/2}} (u - \sin u) \end{aligned} \right\} \Omega_k(r) < 0 \quad (15)$$

$$a(r, t) = \left(\frac{3}{2} H_0(r) (t - t_B(r)) \right)^{2/3} \quad \Omega_k(r) = 0 \quad (16)$$

where $\eta = \eta(r, t)$ and $u = u(r, t)$ are dimensionless parameters related to the conformal time, while $t_B(r)$ is the Big Bang time of a given shell. We choose a homogeneous age of the Universe (in particular, $t_B(r) \equiv 0$), as it has been shown that Big Bang time different from shell to shell introduces decaying modes (Zibin 2008), which in turn implies large CMB spectral distortions (Zibin 2011). In the second simple case of the flat Universe $\Omega_k(r) \equiv 0$ we find a solution:

$$a(r, t) = \sqrt[3]{\frac{\Omega_m(r)}{\Omega_{\Lambda}(r)} \sinh^2 \left[\frac{3}{2} H_0(r) t \sqrt{\Omega_{\Lambda}(r)} \right]} \quad (17)$$

Obviously, as $\Omega_k(r) \equiv 0$, the profile of the Λ term is defined by the profile of matter density. Note that this case recovers the Λ CDM model for $\Omega_m(r) \equiv \text{const}$. In this work, we will consider LTB models with a specific matter density profile:

$$\Omega_m(r) = \Omega_{\text{out}} - (\Omega_{\text{out}} - \Omega_{\text{in}}) e^{-r^2/2\rho^2}, \quad (18)$$

where $\Omega_{\text{in}} \leq \Omega_{\text{out}}$ are the density parameters at the centre and outside of this underdensity (also called *void*), while the parameter ρ defines its size. Clearly for $r \rightarrow \infty$ we recover a FLRW model with $\Omega_m = \Omega_{\text{out}}$. In fact, we will fix the value of Ω_{out} to unity in order to be consistent with the inflationary paradigm. This simple density profile provides a smooth transition from the local to the distant matter density, without introducing too many free parameters. Furthermore, we assume the observer to be located at the centre of the void. This is obviously a privileged position, against the Copernican principle, but the assumption can be relaxed with some complication of the mathematical formalism (Alnes & Amarzguioui 2006). We will address these issues in a forthcoming paper.

The two physical observables of interest, radial cosmic expansion rate and luminosity distance, are derived from observation of photons that are arriving radially in the chosen reference frame. Therefore, we are using the relation of the two independent coordinates r and t with the redshift z along the radial null geodesic (Enqvist & Mattsson 2007)

$$\frac{dr}{dz} = \frac{c \sqrt{1 - k(r)}}{(1 + z) \dot{R}(r, t)} \quad (19)$$

$$\frac{dt}{dz} = -\frac{R'(r, t)}{(1 + z) \dot{R}(r, t)} \quad (20)$$

Finally, the solutions of Eqs. (19) and (20) can be used in combination with Eqs. (10) and (11) to relate any observable as a function of the redshift. The luminosity and the angular diameter distances in LTB model (see Ellis (2007)) are given by

$$d_A(z) = R(r(z), t(z)), \quad d_L(z) = (1 + z)^2 d_A(z) \quad (21)$$

and can be calculated numerically as functions of the redshift using the equations above.

3. Data analysis: methods

We want to test the theoretical models described in Section 2 against a number of independent observables that are SN Ia, OHD and BAO. Our goal is to address specifically the H_0 determination out of these measurements, also discussing the estimates of the other cosmological parameters. We perform an analysis for each of the datasets separately, and then a joint analysis to improve the sensitivity of our estimates.

3.1. SN Ia

The first dataset we consider is the JLA sample of SN Ia, for the reason already explained in the introduction. Once a SN Ia is identified, the raw measurements are corrected for the galactic extinction and the cross-filter change from observed band to the SN rest-frame B band. The JLA catalogue is built by processing these data with the use of the SALT light curve and spectral fitters (Guy et al. 2007), which provide the data points that can further be used in a cosmological study. Each SN is characterised by its redshift z , the value for the maximum B-band apparent magnitude m_B , then stretch and colour correction factors, s and c , respectively. Although considered the best-known high-redshift standard candles in cosmology, SN Ia still show small variations in their maximum absolute luminosity, and hence, in the B-band absolute magnitude, M_B . To take this into account, the maximum absolute magnitude has been so far corrected through the empirical relation

$$M_B^{\text{corr}} = M_B - \alpha s + \beta c, \quad (22)$$

where M_B^{corr} and the two correction parameters, α and β , are assumed to be constant for all the SN Ia (Hamuy et al. 1995; Kasen & Woosley 2007). Comparison with the cosmological models is done by using the distance modulus $\mu \equiv m_B - M_B$ that is related to the luminosity distance, $d_L = d_H D_L$. Here, $d_H \equiv c/H_0 \approx 3000h^{-1}\text{Mpc}$ is the Hubble radius, while D_L is a ‘‘Hubble constant-free’’ dimensionless luminosity distance, which depends on the other cosmological parameters. Therefore, the $\mu - d_L$ relation can be written as follows

$$m_B - M_B^{\text{corr}} + \alpha s - \beta c = 5 \log_{10} d_H + 5 \log_{10} D_L + 25 \quad (23)$$

This equation has been so far used to fit at once the three nuisance parameters (α , β and $\mathcal{M} \equiv M_B^{\text{corr}} + 5 \log_{10} d_H$) together with the cosmological parameters relevant for the calculation of $D_L(z)$. It is evident that the distance moduli provided in SN datasets, depending on such estimates of the nuisance parameters, are consequently biased due to the pre-assumption of the Λ CDM model. It follows from the definition of \mathcal{M} that the estimates of the cosmological parameters are insensitive to the actual value of H_0 , which plays the role of an overall offset in Eq. (23).

Assuming α , β and M_B^{corr} as constant means that every SN has the same corrected absolute magnitude and that no further corrections are needed. This statement has been questioned by Trøst Nielsen et al. (2015), who extend the procedure to consider the variation of the corrected absolute magnitude M_B^{corr} from one to another SN. For the sake of simplicity, M_B^{corr} , s and c are assumed to be independent Gaussian variables with Normal distributions $\mathcal{N}(M_0, \sigma_{M_0})$, $\mathcal{N}(s_0, \sigma_{s_0})$ and $\mathcal{N}(c_0, \sigma_{c_0})$, respectively. On the contrary, α and β are still considered constant coefficients of Eq. (22). Here we follow the same approach. Therefore, the joint probability for the values of the intrinsic SN parameters can be written as

$$p(Y) = |2\pi\Sigma_I|^{-1/2} \exp[-(Y - Y_0)\Sigma_I^{-1}(Y - Y_0)^T/2], \quad (24)$$

where $Y = (M_1, s_1, c_1, \dots, M_N, s_N, c_N)$ is a $3N$ -vector of the true values of the intrinsic parameters for each of the N supernovae; $Y_0 = (M_0, s_0, c_0, \dots, M_0, s_0, c_0)$ is a $3N$ -vector with the central values of the parameters’ distributions; $\Sigma_I = \text{diag}(\sigma_{M_0}^2, \sigma_{s_0}^2, \sigma_{c_0}^2, \dots, \sigma_{M_0}^2, \sigma_{s_0}^2, \sigma_{c_0}^2)$ is the $3N \times 3N$ covariance matrix. The measured values (\hat{m}_B , \hat{s} , \hat{c}) are conveniently expressed with the $3N$ -vector $\hat{Z} = (\hat{m}_{B1} - \mu_1, \hat{s}_1, \hat{c}_1, \dots)$. Following

Trøst Nielsen et al. (2015), we define as θ the full set of free parameters, which describe both the astrophysical properties of SN and the cosmology. Then, the Likelihood of the observed values, given the theoretical model θ , can be conveniently written as:

$$\mathcal{L}_{\text{SN}}(\hat{Z}|\theta) = |2\pi(\Sigma_d + A^T\Sigma_I A)|^{-1/2} \times \exp[-(\hat{Z} - Y_0 A)(\Sigma_d + A^T\Sigma_I A)^{-1}(\hat{Z} - Y_0 A)^T/2], \quad (25)$$

where Σ_d is the covariance matrix of the data (Betoule et al. 2014), and A is the $3N \times 3N$ block-diagonal matrix

$$A = \begin{pmatrix} 1 & 0 & 0 \\ -\alpha & 1 & 0 \\ \beta & 0 & 1 \\ & & \ddots \end{pmatrix}. \quad (26)$$

In analysing the JLA dataset by itself, we do not assume any prior on H_0 , as we estimate the total offset \mathcal{M} . Note that the distribution $\mathcal{N}(M_0, \sigma_{M_0})$ implies the distribution of \mathcal{M} : $\mathcal{N}(\mathcal{M}_0, \sigma_{\mathcal{M}_0})$, with $\sigma_{\mathcal{M}_0} = \sigma_{M_0}$ and $\mathcal{M}_0 = M_0 + 5 \log d_H$. Hence, using this method there are 8 parameters describing the physics of SN Ia: α , β , M_0 , σ_{M_0} , s_0 , σ_{s_0} , c_0 , σ_{c_0} (instead of 3 as in the conventional approach), which need to be fitted simultaneously with the cosmological parameters.

3.2. OHD

We have seen in Section 2. that the radial cosmic expansion rate is proportional to dz/dt , both for FLRW models (cf. Eq. (2)) and for LTB models (cf. Eqs. (10) and (20)). Therefore, by measuring the age difference of two objects at two close redshift points, one can estimate the radial expansion rate at the corresponding redshift. For this purpose, Jimenez & Loeb (2002) proposed what is called the differential age (DA) method, which uses pairs of passively-evolving red galaxies found at very similar redshifts. Another way to determine the expansion history of the Universe is by using BAO (Gaztañaga et al. 2009; Delubac et al. 2015; Sahni et al. 2014). In the present work we use only the 23 DA points from the dataset collected and updated by Ding et al. (2015). The shape of the $H(z)$ curve constrains the cosmological models, while the offset value provides us with the local cosmic expansion rate, H_0 . For this dataset, we perform a simple Likelihood analysis considering that all the data points are uncorrelated:

$$\mathcal{L}_{\text{OHD}} \propto \exp\left[-\frac{1}{2} \sum_{i=1}^{23} \left(\frac{\hat{H}_i - H(z_i)}{\sigma_{H_i}}\right)^2\right] \quad (27)$$

Here \hat{H}_i is the observed value at redshift z_i with its own uncertainty σ_{H_i} . As far as theoretical prediction is concerned, we use for $H(z_i)$ either Eq. (3) for the FLRW models or Eq. (10) for LTB cosmologies.

3.3. BAO

The large-scale structure of the Universe has been extensively studied via redshift surveys, such as the 6-degree field galaxy survey-6dFGS (Beutler et al. 2011) and the Sloan Digital Sky Survey-SDSS (Gil-Marín et al. 2015). The estimated galaxy correlation function shows a peak at large scales which is interpreted as the signature of the baryon acoustic oscillation in the relativistic plasma of the early Universe. In FLRW cosmology,

the acoustic-scale distance ratio is defined by $\Xi \equiv r_d/D_V(z)$, where

$$r_d = \int_{z_d}^{\infty} \frac{c_s(z)}{H(z)} dz \quad (28)$$

is the comoving sound horizon at the redshift z_d of the baryon drag epoch (Eisenstein et al. 1998) and

$$D_V(z) \equiv \left[(1+z)^2 d_A^2(z) \frac{cz}{H(z)} \right]^{1/3} \quad (29)$$

is a spherically averaged distance measure introduced by Eisenstein et al. (2005). In LTB cosmology, structure formation is poorly understood and this is why the use of the BAO data for this model is still controversial (Zibin 2008; Clarkson et al. 2009).

In this paper, we use the measurements from the 6dFGS (Beutler et al. 2011), the SDSS DR7 (Ross et al. 2015), the BOSS DR11 (Anderson et al. 2014) samples and the Ly α forest measurements from BOSS DR11 (Delubac et al. 2015; Font-Ribera et al. 2014). The 6dFGS sample we use contains 75,117 galaxies up to $z < 0.15$ and gives $r_d/D_V = 0.336 \pm 0.015$ at an effective redshift $z_{eff} = 0.106$. The SDSS DR7 catalogue contains 63,163 galaxies at $z < 0.2$ and the measurement given is $D_V(z_{eff} = 0.15) = (664 \pm 25)(r_d/r_{d, fid})$ Mpc, where $r_{d, fid} = 148.69$ Mpc in their fiducial cosmology. BOSS DR11 contains nearly one million galaxies in the redshift range $0.2 < z < 0.7$ and the two measurements given are $D_V(z_{eff} = 0.32) = (1264 \pm 25)(r_d/r_{d, fid})$ Mpc and $D_V(z_{eff} = 0.57) = (2056 \pm 20)(r_d/r_{d, fid})$ Mpc with $r_{d, fid} = 149.29$ Mpc. The Ly α forest of BOSS DR11 consists of 137,562 quasars in the redshift range $2.1 \leq z \leq 3.5$ and provides $d_A/r_d = 11.28 \pm 0.65$, $d_H/r_d = 9.18 \pm 0.28$ at $z_{eff} = 2.34$, and $d_A/r_d = 10.8 \pm 0.4$, $d_H/r_d = 9.0 \pm 0.3$ at $z_{eff} = 2.36$, where $d_H(z) = c/H(z)$. In order to unify the measured BAO quantity as $r_d/D_V(z)$, we invert the results of SDSS DR7 and BOSS DR11 using their fiducial values $r_{d, fid}$, and combine the measurements of Ly α forest from BOSS DR11 by means of Eq. (29). The observed values $\hat{\Xi}(z) \equiv r_d/D_V(z)$ used in this paper are shown in Table 1.

Table 1. BAO data used in this work.

z	$\hat{\Xi}$	σ_{Ξ}	Ref.
0.106	0.336	0.015	Beutler et al. (2011)
0.15	0.2239	0.0084	Ross et al. (2015)
0.32	0.1181	0.0023	Anderson et al. (2014)
0.57	0.0726	0.0007	Anderson et al. (2014)
2.34	0.0320	0.0016	Delubac et al. (2015)
2.36	0.0329	0.0012	Font-Ribera et al. (2014)

The acoustic scale has also been measured by Kazin et al. (2014) using the WiggleZ galaxy survey. They report three correlated measurements at redshifts 0.44, 0.60 and 0.73. However, we decide not to use these measurements in this paper, since the WiggleZ volume partially overlaps that of the BOSS sample and the correlations between the two surveys have not been quantified.

As all the BAO data points in Table 1 are uncorrelated, we perform a simple Likelihood analysis:

$$\mathcal{L}_{\text{BAO}} \propto \exp \left[-\frac{1}{2} \sum_{i=1}^6 \left(\frac{\hat{\Xi}_i - \Xi(z_i)}{\sigma_{\Xi_i}} \right)^2 \right] \quad (30)$$

Here $\hat{\Xi}_i$ is the observed value at redshift z_i with its own uncertainty σ_{Ξ_i} (see Table 1). The theoretical estimate, $\Xi(z_i)$, has been evaluated using Eqs. (28) and (29) and by exploiting the fitting formula for z_d given in Eisenstein et al. (1998).

3.4. Combined analysis

As we will show in the next Section, each of the three datasets considered in this paper are providing good estimates of the cosmological parameters. However, it is worth to combine all the three datasets to obtain more robust constraints. Moreover, the joint analysis allows us to provide separate estimates for the SN absolute magnitude and the Hubble constant. Assuming that the three datasets are independent, we evaluate the total Likelihood as the product of the Likelihoods of the single datasets. Therefore, for FLRW models $\mathcal{L}_{\text{tot}} = \mathcal{L}_{\text{SN}} \mathcal{L}_{\text{OHD}} \mathcal{L}_{\text{BAO}}$, while for LTB cosmologies $\mathcal{L}_{\text{tot}} = \mathcal{L}_{\text{SN}} \mathcal{L}_{\text{OHD}}$ as in this case we do not consider the BAO dataset.

4. Data analysis: results

We present the results for cosmological models based on the FLRW metric and the LTB one as well. A number of FLRW models have been analysed by Trøst Nielsen et al. (2015) using the JLA dataset and we fully agree with their results. We extend their discussion including the w CDM and LTB models, and also present the constraints coming from the OHD and the BAO datasets. The JLA, OHD and BAO data strongly constrain the apparent acceleration of the cosmic expansion, the present expansion rate and the curvature of the Universe, respectively. A joint analysis, then, allows us to see what improvement we may have in the estimation of the cosmological parameters.

4.1. Constraints on flat Λ CDM model

The flat Λ CDM model has been so far tested with the available cosmological observables and it is commonly considered the concordance model in cosmology. The results of our analy-

Table 2. Results from the fits of the Λ CDM model to the data.

Data	H_0 [km/s/Mpc]	Ω_m	$\Omega_\Lambda = 1 - \Omega_m$
JLA	-	0.376 ± 0.031	0.624 ± 0.031
OHD	68.7 ± 3.3	0.319 ± 0.061	0.681 ± 0.061
BAO	67.3 ± 2.2	0.334 ± 0.042	0.689 ± 0.037
JLA+OHD	66.7 ± 2.0	0.366 ± 0.028	0.634 ± 0.028
JLA+OHD+BAO	67.8 ± 1.0	0.350 ± 0.016	0.650 ± 0.016

sis for this model are presented in Table 2. In particular, using the JLA dataset alone we reproduce the Ω_m value found by Trøst Nielsen et al. (2015). In addition to their results, we also quote the uncertainties in the parameter estimates, which show that the JLA dataset provides consistent results with the ones we find for OHD and BAO samples. However, our values for Ω_m , obtained from JLA only and JLA+OHD+BAO, are both about 1.9σ away from the most recent determination of Planck (TT, TE, EE + lowP) that provides $\Omega_m = 0.316 \pm 0.009$.

Concerning the present expansion rate, the H_0 estimates coming from the OHD and BAO data are consistent between themselves and with Planck. The JLA dataset by itself is insensitive to H_0 . However, in the joint analysis JLA constrains other parameters of the fit, which in turn affect the estimate of H_0 . It turns out that the final value for H_0 coming from the joint

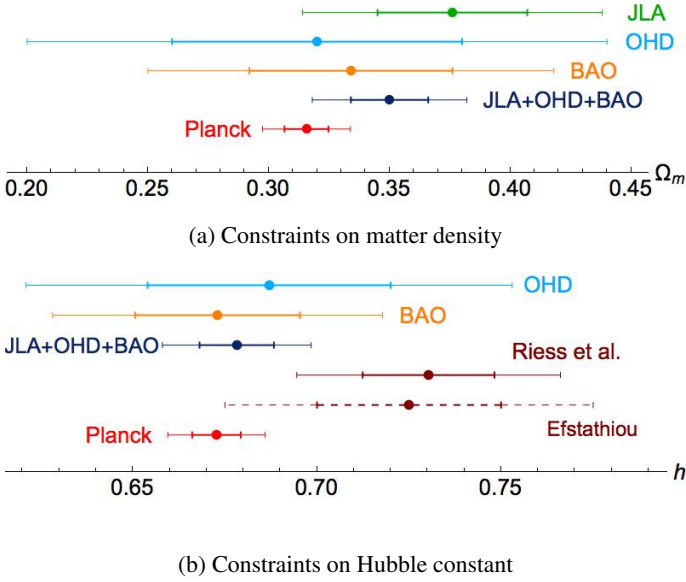


Fig. 1. Results at the 1σ and 2σ c.l. for the parameters of the Λ CDM model when fitted to: JLA (green), OHD (azure), BAO (orange) and the three datasets combined (dark blue). Constraints from the direct measurement by Riess et al. (2016) (dark red), the reanalysis by Efstathiou (2014) (dashed dark red) and the Planck Collaboration (2015) (red) are also shown.

JLA+OHD+BAO analysis is in excellent agreement with the one from Planck (Figure 1), but still 1.7σ and 2.5σ away from the findings by Efstathiou (2014) and Riess et al. (2016).

4.2. Constraints on $k\Lambda$ CDM model

This model is completely defined by the three cosmological parameters: H_0 , Ω_m and Ω_Λ . The best-fit values together with their statistical errors in Table 3 show a clear consistency among the results obtained by analysing the single datasets. We present the

Table 3. Results from the fits of the $k\Lambda$ CDM model to the data.

Data	H_0 [km/s/Mpc]	Ω_m	Ω_Λ
JLA	-	0.341 ± 0.098	0.569 ± 0.149
OHD	68.2 ± 5.7	0.291 ± 0.265	0.622 ± 0.539
BAO	68.7 ± 7.3	0.354 ± 0.106	0.646 ± 0.106
JLA+OHD	66.3 ± 2.2	0.319 ± 0.044	0.556 ± 0.144
JLA+OHD+BAO	68.1 ± 1.0	0.350 ± 0.016	0.650 ± 0.016

confidence regions for the $k\Lambda$ CDM model in Figure 2. Our results show that the BAO data constrain quite strictly the curvature of the Universe to be zero, leading to a strong correlation between Ω_m and Ω_Λ and shrinking the confidence regions to a line in $\Omega_m - \Omega_\Lambda$ plane. An alternative way to study the BAO data is by parametrising the $k\Lambda$ CDM model with Ω_m and Ω_k . In this case, the result for Ω_m will be the same as in Table 3, while the best-fit value of Ω_k is vanishingly small and consistent with zero. This is why the best-fit values of H_0 and Ω_m are not exactly the same as the ones obtained in Λ CDM case (c.f. Table 2), although in a very good agreement. The constraints from the JLA and OHD samples are fully consistent with the flat cosmology, although the best fit values are slightly off this line. The confidence regions in the $\Omega_m - h$ and $h - \Omega_\Lambda$ planes, resulting from the OHD and BAO data, fully overlap. In fact, the estimates for H_0 coming from the BAO and OHD analysis are consistent among

themselves (see Table 3). Note that in our full joint analysis, the $k\Lambda$ CDM and the Λ CDM models provide almost the same parameter estimates.

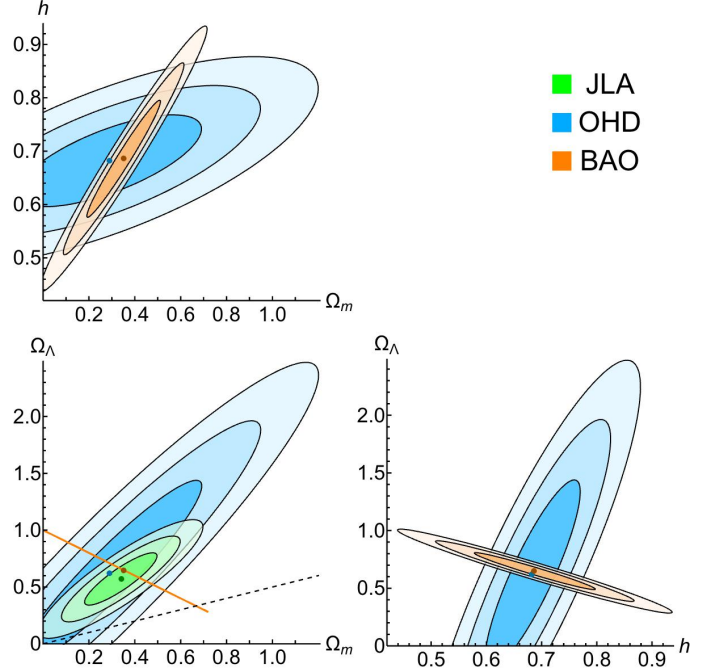


Fig. 2. 1σ , 2σ and 3σ confidence regions resulting from the fit of $k\Lambda$ CDM model to the single datasets as indicated in the top-right panel. The dashed line in the $\Omega_m - \Omega_\Lambda$ plane represents the transition from the decelerating (below) to the accelerating (above) models.

4.3. Constraints on w CDM model

The w CDM model considers a DE fluid with a free EoS parameter w , instead of a constant Λ term corresponding to $w = -1$. The addition of one more parameter implies larger error bars in the Ω_m and H_0 determinations presented in Table 4. The con-

Table 4. Results from the fits of the w CDM model to the data.

Data	H_0 [km/s/Mpc]	Ω_m	w
JLA	-	0.347 ± 0.119	-0.92 ± 0.30
OHD	68.5 ± 7.2	0.318 ± 0.077	-0.98 ± 0.69
BAO	65.5 ± 8.0	0.329 ± 0.049	-0.93 ± 0.28
JLA+OHD	67.0 ± 1.9	0.318 ± 0.073	-0.86 ± 0.17
JLA+OHD+BAO	66.5 ± 1.8	0.346 ± 0.017	-0.93 ± 0.07

confidence regions in Figure 3 show a clear agreement among the results derived from the single datasets, although with different uncertainties. In particular, the estimates of w are consistent with $w = -1$, the Λ CDM model. The value of Ω_m resulting from the full joint analysis is very close to the one obtained for the Λ CDM model. The OHD and BAO estimates of H_0 are not very well constrained. However, again, the joint JLA+OHD+BAO analysis provides a value of H_0 that is 1.7σ and 2.6σ away from the results of Efstathiou (2014) and Riess et al. (2016), respectively.

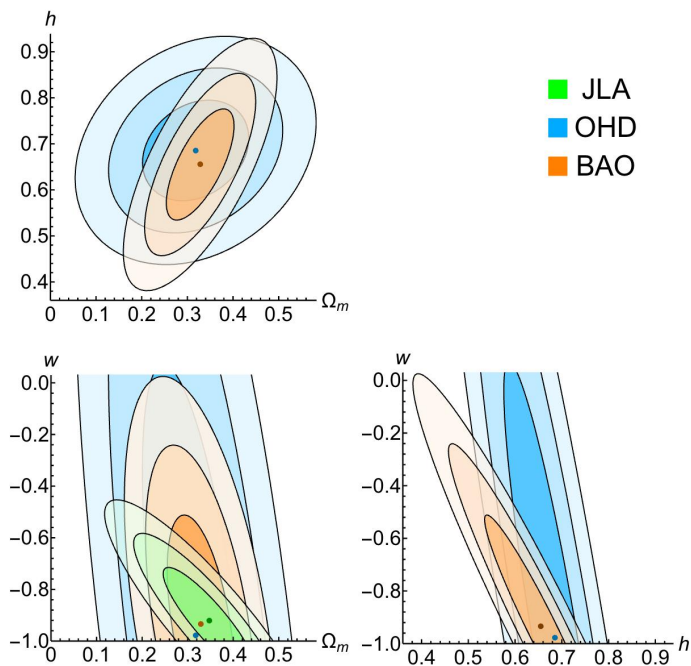


Fig. 3. 1σ , 2σ and 3σ confidence regions from the fits of the w CDM model to the single datasets as indicated in the top-right panel.

4.4. Constraints on LTB model

Here we extend the discussion of Trøst Nielsen et al. (2015) to consider LTB models. In the LTB model, the apparent acceleration of the local Universe arises from the fact that the matter density decreases radially from high to local redshifts. The radial matter density profile is in our case completely defined by Eq. (18), where we fix $\Omega_{\text{out}} = 1$ and the remaining free parameters are the local value of the matter density Ω_{in} and the dimensionless parameter ρ , related to the size of the void. For the JLA data, these two are the only cosmological parameters in the fit, as H_0 is included in the offset \mathcal{M} . Instead, for the OHD data we can fit all the three cosmological parameters. The JLA sample

Table 5. Results from the fits of the LTB model to the data.

Data	H_0 [km/s/Mpc]	Ω_{in}	ρ
JLA	-	0.228 ± 0.046	0.61 ± 0.13
OHD	64.1 ± 3.1	0.151 ± 0.073	1.23 ± 0.54
JLA+OHD	64.2 ± 1.9	0.174 ± 0.038	0.86 ± 0.19

constrains Ω_{in} to be about a quarter of the critical density, while the value resulting from the OHD dataset is lower, but in agreement within the errors (cf. Table 5). In order to have a feeling about the physical size of the void, one should look at the comoving angular diameter distance $R_0(r = \rho) = c t_0 \rho$. The age of the Universe, t_0 , in the LTB model is related to H_0 through Eq. (14). Hence, we evaluate the angular diameter distance using $H_0 = 100 \text{ km s}^{-1}/\text{Mpc} \times h$. For the ρ best-fit value from the JLA analysis we get $R_0(r = \rho) \approx 2.5 \text{ Gpc}/h$. The OHD analysis aims to a much larger void, but with a void profile consistent within the errors with the JLA data (see Figure 4). We similarly perform a joint JLA+OHD analysis for the LTB model. The H_0 best-fit value is lower than the one obtained for Λ CDM. This characteristic of LTB models has been observed in earlier works: our H_0 estimate is consistent within 2σ with the findings of Nadathur &

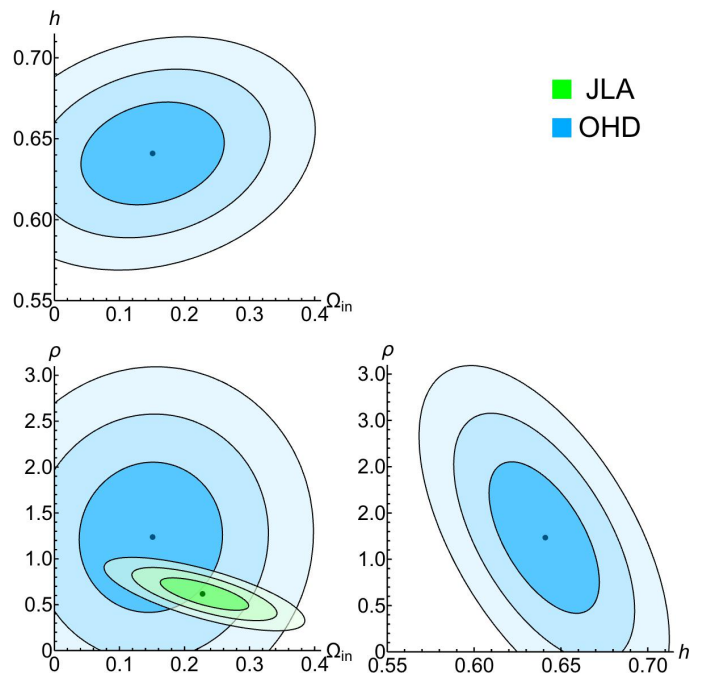


Fig. 4. 1σ , 2σ and 3σ confidence regions for the LTB model to the single datasets as indicated in the top-right panel.

Sarkar (2011) and at the 1σ level with the value from Freedman et al. (2001). However, our value is 2.6σ away from the result of Efstathiou (2014) and 3.4σ away from the value given by Riess et al. (2016), which is an even higher tension than in the case of the Λ CDM model. In our analysis we also consider the Λ LTB model, as an extension of the LTB one, and find that it converges to Λ CDM model using both JLA and OHD datasets (see Table 6). In fact, the best-fit value of Ω_{in} is equal to Ω_m obtained for Λ CDM, while the size of the void tends to infinity.

Table 6. Results from the fits of the Λ LTB model to the data.

Data	H_0 [km/s/Mpc]	Ω_{in}	ρ
JLA	-	0.376 ± 0.031	∞
OHD	68.7 ± 3.3	0.319 ± 0.061	∞
JLA+OHD	66.7 ± 2.0	0.366 ± 0.028	∞

In order to better compare the considered cosmologies we use the Akaike information criterion (AIC) and Bayes factor (K). The Akaike estimate of minimum information (Akaike 1974) for a given theoretical model and a given dataset is defined as

$$\text{AIC} = -2 \log \mathcal{L}^{\text{max}} + 2p \quad (31)$$

where p is the number of independent parameters. By definition, this test gives preference to the model with the lowest AIC. In Table 7 we present the differences, $\Delta(\text{AIC})$, of the AIC values between each theoretical scenario and Λ CDM. The Bayes factor similarly provides a criterion for choosing between two models by comparing their best likelihood values. In fact, the Bayes factor, $K = \mathcal{L}_{M_1}^{\text{max}} / \mathcal{L}_{M_2}^{\text{max}}$ represents the "odds" for the model M_1 against the alternative model M_2 . It is commonly considered that odds lower than 1:10 indicate a strong evidence against M_1 (Jeffreys 1983). In reversed reading, odds greater than 10 : 1 indicate a strong evidence against M_2 . In Table 7 we also show the Bayes factor of every model considered in this work against Λ CDM. The standard Λ CDM model is preferred by the Akaike criterion

Table 7. Comparison of the cosmological models by $\Delta(\text{AIC}) = \text{AIC}_X - \text{AIC}_{\Lambda\text{CDM}}$ and $K = \mathcal{L}_{\Lambda\text{CDM}}^{\text{max}}/\mathcal{L}_X^{\text{max}}$, using the combined analysis JLA+OHD.

Model X	$\Delta(\text{AIC})$	K
ΛCDM	0	1
$k\Lambda\text{CDM}$	1.69	1 : 1.17
$w\text{CDM}$	1.40	1 : 1.35
LTB	9.41	40 : 1
ΛLTB	2	1

for fitting the JLA+OHD data. We note that both $k\Lambda\text{CDM}$ and $w\text{CDM}$ models have an extra parameter with respect to ΛCDM . Nevertheless, the latter has still a lower AIC value, since the Akaike criterion rewards the model with less parameters. It turns out that the LTB model is strongly disfavoured with respect to ΛCDM by both the AIC criterion and the Bayes factor. This behaviour mostly arises from the SN data. In fact, from our fit to the OHD data alone we get $-2 \log \mathcal{L}$ values of 12.91 and 12.56 for LTB and ΛCDM , concluding that LTB can be used to fit OHD data, as found by Wang & Zhang (2012). However, after using the JLA dataset alone with the Trøst Nielsen et al. (2015) approach we get $-2 \log \mathcal{L}$ values of -209.88 and -214.83 for the LTB and ΛCDM models, respectively. We then conclude that the LTB model is not performing as good as the concordance one in fitting the SN Ia data. This is opposite to the previous findings in the literature (Alnes et al. 2006; Garfinkle 2006; Blomqvist & Mörtzell 2010), and consistent with the work by Vargas et al. (2015).

4.5. SN Ia intrinsic parameters

When performing the combined analysis, we are able to fit at once all the cosmological parameters and the eight intrinsic astrophysical parameters of SN Ia. The latter are those characterising the normal distributions $\mathcal{N}(M_0, \sigma_{M_0})$, $\mathcal{N}(s_0, \sigma_{s_0})$ and $\mathcal{N}(c_0, \sigma_{c_0})$, and the constant coefficients α and β of Eq. (22). As an example, in Table 8 we present estimates of these nu-

Table 8. Results for the SN Ia intrinsic parameters from the combined JLA+OHD+BAO fit of the standard ΛCDM model.

M_0	σ_{M_0}	s_0	σ_{s_0}
-19.13 ± 0.04	0.108 ± 0.005	0.038 ± 0.038	0.932 ± 0.027
c_0	σ_{c_0}	α	β
-0.016 ± 0.005	0.071 ± 0.002	0.134 ± 0.006	3.059 ± 0.087

sance parameters in the case of the ΛCDM model, resulting from a combined fit with all the three datasets. The peak luminosity of SN does not have a constant value even after the corrections for the stretch and the colour factors: the variation of the corrected SN Ia absolute magnitude is about 0.22 at the 2σ level. Besides light curve shape and colour, peak luminosity was similarly correlated to other parameters, including the host galaxy mass and the metallicity (Kelly et al. 2010; Hayden et al. 2013). Even these effects can be naturally taken into account in the distribution $\mathcal{N}(M_0, \sigma_{M_0})$, considering that any additional correlations should shrink the distribution width. Interestingly enough, the best-fit results of the SN parameters seem to be independent on the cosmological model under consideration: changing the model introduces, at most, variations on the last significant digit in the numbers given in Table 8. The only exception is the central

value of $\mathcal{N}(M_0, \sigma_{M_0})$ obtained from the combined JLA+OHD fit for the LTB model: $M_0 = -19.21 \pm 0.06$. This is due to the lower value of H_0 resulting from the fit to the OHD data.

5. Indirect H_0 estimates

The estimates of the Hubble constant from our joint analysis and from WMAP and Planck are shown in Figure 5 together with the most recent direct estimates by Efstathiou (2014) and Riess et al. (2016). It is worth stressing the excellent agreement between our value of H_0 for ΛCDM and the CMB-only Planck measurement. Note also the consistency of the results we obtained for different FLRW cosmologies. On the other hand, as already said, the value of H_0 in LTB is lower than those of the FLRW models.

The indirect estimates of H_0 result to be systematically lower than the direct estimates. The best-fit values of H_0 for the ΛCDM and the LTB models are: 1.7σ and 2.6σ away from the value presented by Efstathiou (2014); 2.5σ and 3.4σ away from the result found by Riess et al. (2016). Concerning ΛCDM , Riess et al. (2016) suggest that an additional source of dark radiation in the early Universe could allow to best-fit the Planck data with a larger value for H_0 . This change would certainly affect the value of the sound horizon and, then, our H_0 estimate from BAO. However, this change cannot affect our result from the JLA+OHD analysis, which remains in 2.4σ tension with Riess et al. (2016) and in complete agreement with Planck. We conclude that this tension cannot be eliminated neither by changing N_{eff} in the concordance model nor by invoking possible systematic uncertainties in the CMB measurements. If this were the case, we couldn't have found a good agreement between our JLA+OHD+BAO result and Planck (TT, TE, EE + lowP).

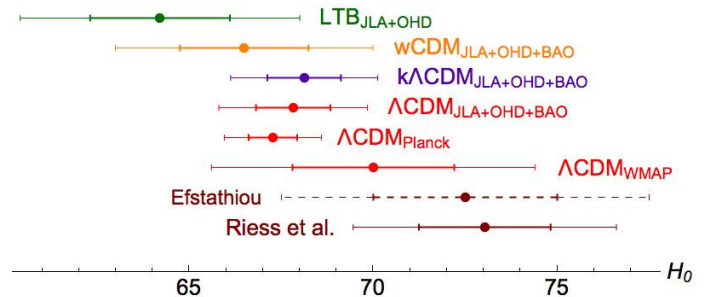


Fig. 5. Results at the 1σ and 2σ c.l. for H_0 , in standard units of $\text{km s}^{-1}/\text{Mpc}$, from our combined analysis for LTB, $w\text{CDM}$, $k\Lambda\text{CDM}$ and ΛCDM models. The results from CMB-only measurements by Planck Collaboration (2015) and Hinshaw et al. (2013), and the direct estimates by Riess et al. (2016) and Efstathiou (2014) are also shown for comparison.

Given the cosmological model, the age of the Universe, t_0 , is completely defined by the H_0 estimates. Here we use the result of our combined analysis for the Hubble constant to compare t_0 with the estimate of the absolute ages of stellar systems (Bono et al. 2010; Monelli et al. 2015). In fact, there is quite a good convergence on the value $t_0 = (13.7 \pm 0.5)$ Gyr from different class of observations (see, for a review, Freedman & Madore (2010)). Therefore, in Figure 6 we show the iso-ages corresponding to 13.2, 13.7 and 14.2 Gyr for both ΛCDM and LTB models. Note that we show the theoretical predictions in the same $\Omega_m^{\text{loc}} - H_0$ plane, where the local matter density Ω_m^{loc} corresponds to Ω_m or to Ω_{in} for the ΛCDM or LTB model, respectively. Our estimates for the age of the Universe coming from the best-fit results of the combined analysis described above are $t_0 = (13.3 \pm 0.4)$ Gyr for ΛCDM and $t_0 = (13.1 \pm 0.7)$ Gyr for LTB. In Figure 6 we

also show the 1σ and 2σ confidence regions resulting from the JLA+OHD+BAO analysis for the Λ CDM model, and those obtained from the JLA+OHD analysis for LTB. These are completely consistent with the observational estimate of t_0 quoted above.

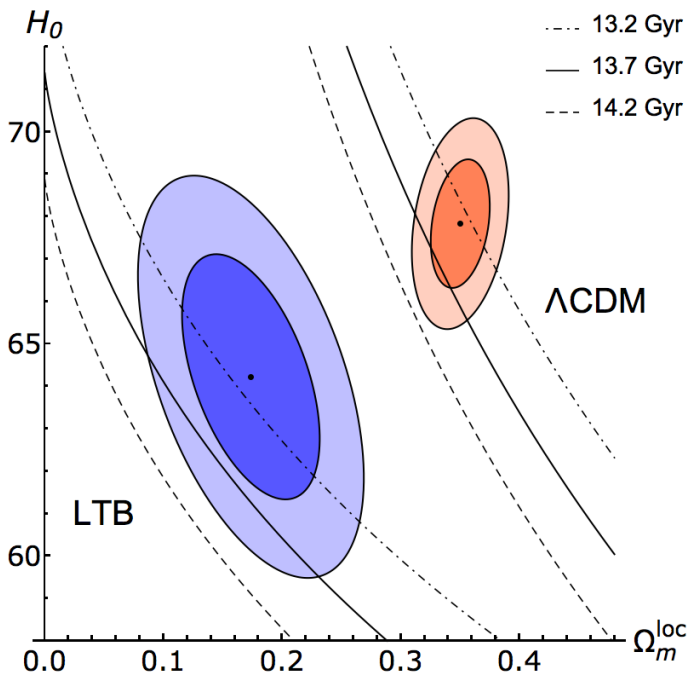


Fig. 6. Theoretical iso-ages for the Λ CDM and LTB models, corresponding to ages of (13.2 ± 0.5) Gyr are shown in the $\Omega_m^{\text{loc}} - H_0$ plane, together with the 1σ and 2σ confidence regions resulting from the joint JLA+OHD+BAO (JLA+OHD) analysis for the Λ CDM (LTB) model.

6. Summary and conclusions

The combined analysis of JLA, OHD and BAO datasets allowed us to reach more robust constraints on the cosmological parameters¹ and to break the degeneracy between the SN absolute magnitude and the cosmic expansion rate. Our main findings can be summarised as follows.

By fitting the cosmological and the SN intrinsic parameters to the combined set of JLA, OHD and BAO data, we constrain the distributions of SN absolute magnitude, stretch and color. The resulting values are cosmological-model independent, with the exception of M_0 value obtained for LTB. The method we use can in principle be extended to include the effects related to mass and metallicity of the host galaxies.

We study the Λ CDM model and its extensions to consider non-vanishing spatial curvature and different assumptions for the dark energy component. The combined analysis clearly prefers the concordance model, as it forces the curvature to vanish and the DE EoS to be consistent with $w = -1$.

We also study a LTB model with a Gaussian profile, which results to be strongly disfavoured with respect to the concordance model by information criteria, such as AIC analysis or Bayes factor.

Concerning the Λ CDM model, the JLA+OHD+BAO analysis provides a value of $H_0 = (67.8 \pm 1.0)$ km s⁻¹/Mpc that is

¹ Our analysis has been implemented in *Mathematica* 10. The code is available upon request.

fully consistent with the Planck (TT, TE, EE + lowP) result. This makes less probable that the tension with the direct measurements by Riess et al. (2016) is due to systematics in the Planck CMB measurements. Also, it seems difficult to reconcile direct and indirect H_0 measurements by considering an additional source of dark radiation in the early Universe, as this would not affect the JLA+OHD fit which is still consistent with Planck. Therefore, the need to go beyond the concordance Λ CDM model remains still an open question.

Acknowledgements. We are grateful to Jeppe Trøst Nielsen for useful discussions on the JLA data analysis, and to Martin White for his advice about the BAO data. We thank Giuseppe Bono and the referee for their constructive comments and helpful suggestions.

References

- Akaike, H. 1974, IEEE Transactions on Automatic Control, 19, 716
Alnes, H. & Amarzguoui, M. 2006, Phys. Rev. D, 74, 103520
Alnes, H., Amarzguoui, M., & Grøn, Ø. 2006, Phys. Rev. D, 73, 083519
Amanullah, R., Lidman, C., Rubin, D., et al. 2010, ApJ, 716, 712
Anderson, L., Aubourg, E., Bailey, S., et al. 2014, MNRAS, 441, 24
Betoule, M., Kessler, R., Guy, J., et al. 2014, A&A, 568, A22
Beutler, F., Blake, C., Colless, M., et al. 2011, MNRAS, 416, 3017
Blomqvist, M. & Mörtzell, E. 2010, J. Cosmology Astropart. Phys., 5, 006
Bondi, H. 1947, MNRAS, 107, 410
Bono, G., Stetson, P. B., VandenBerg, D. A., et al. 2010, ApJ, 708, L74
Cheng, C. & Huang, Q. 2015, Science China Physics, Mechanics, and Astronomy, 58, 095684
Clarkson, C., Clifton, T., & February, S. 2009, J. Cosmology Astropart. Phys., 6, 25
Delubac, T., Bautista, J. E., Busca, N. G., et al. 2015, A&A, 574, A59
Ding, X., Biesiada, M., Cao, S., Li, Z., & Zhu, Z.-H. 2015, ApJ, 803, L22
Efstathiou, G. 2014, MNRAS, 440, 1138
Eisenstein, D. J., Hu, W., & Tegmark, M. 1998, ApJ, 504, L57
Eisenstein, D. J., Zehavi, I., Hogg, D. W., et al. 2005, ApJ, 633, 560
Ellis, G. F. R. 2007, General Relativity and Gravitation, 39, 1047
Enqvist, K. & Mattsson, T. 2007, J. Cosmology Astropart. Phys., 2, 19
Font-Ribera, A., Kirkby, D., Busca, N., et al. 2014, J. Cosmology Astropart. Phys., 5, 27
Freedman, W. L. & Madore, B. F. 2010, ARA&A, 48, 673
Freedman, W. L., Madore, B. F., Gibson, B. K., et al. 2001, ApJ, 553, 47
Friedmann, A. 1922, Zeitschrift für Physik, 10, 377
Friedmann, A. 1924, Zeitschrift für Physik, 21, 326
Garfinkle, D. 2006, Classical and Quantum Gravity, 23, 4811
Gaztañaga, E., Cabré, A., & Hui, L. 2009, MNRAS, 399, 1663
Gil-Marín, H., Percival, W. J., Cuesta, A. J., et al. 2015, ArXiv e-prints
Guy, J., Astier, P., Baumont, S., et al. 2007, A&A, 466, 11
Hamuy, M., Phillips, M. M., Maza, J., et al. 1995, AJ, 109, 1
Hayden, B. T., Gupta, R. R., Garnavich, P. M., et al. 2013, ApJ, 764, 191
Hicken, M., Wood-Vasey, W. M., Blondin, S., et al. 2009, ApJ, 700, 1097
Hinshaw, G., Larson, D., Komatsu, E., et al. 2013, ApJS, 208, 19
Hubble, E. 1929, Proceedings of the National Academy of Science, 15, 168
Jeffreys, H. S. 1983, Theory of probability, The International series of monographs on physics (Oxford: Clarendon Press New York), autre(s) tirage(s) : 1985
Jimenez, R. & Loeb, A. 2002, ApJ, 573, 37
Kasen, D. & Woosley, S. E. 2007, ApJ, 656, 661
Kazin, E. A., Koda, J., Blake, C., et al. 2014, MNRAS, 441, 3524
Kelly, P. L., Hicken, M., Burke, D. L., Mandel, K. S., & Kirshner, R. P. 2010, ApJ, 715, 743
Kirshner, R. P. 2003, Proceedings of the National Academy of Science, 101, 8
Kraśniński, A. 1997, Inhomogeneous Cosmological Models (Cambridge University Press), cambridge Books Online
Lemaître, G. 1933, Annales de la Société Scientifique de Bruxelles, 53, 51
Liu, Z.-E., Qin, H.-F., Zhang, T.-J., Wang, B.-Q., & Bi, S.-L. 2015, ArXiv e-prints
Monelli, M., Testa, V., Bono, G., et al. 2015, ApJ, 812, 25
Nadathur, S. & Sarkar, S. 2011, Phys. Rev. D, 83, 063506
Perlmutter, S., Aldering, G., Goldhaber, G., et al. 1999, ApJ, 517, 565
Planck Collaboration. 2015, ArXiv e-prints
Riess, A. G., Filippenko, A. V., Challis, P., et al. 1998, AJ, 116, 1009
Riess, A. G., Macri, L., Casertano, S., et al. 2011, ApJ, 730, 119
Riess, A. G., Macri, L. M., Hoffmann, S. L., et al. 2016, ArXiv e-prints
Robertson, H. P. 1935, ApJ, 82, 284
Ross, A. J., Samushia, L., Howlett, C., et al. 2015, MNRAS, 449, 835
Sahni, V., Shafieloo, A., & Starobinsky, A. A. 2014, ApJ, 793, L40
Suzuki, N., Rubin, D., Lidman, C., et al. 2012, ApJ, 746, 85
Tolman, R. C. 1934, Proceedings of the National Academy of Science, 20, 169
Trøst Nielsen, J., Guffanti, A., & Sarkar, S. 2015, ArXiv e-prints
Vargas, C. Z., Falciano, F. T., & Reis, R. R. 2015, ArXiv e-prints
Walker, A. G. 1937, Proceedings of the London Mathematical Society, s2-42, 90
Wang, H. & Zhang, T.-J. 2012, ApJ, 748, 111
Zibin, J. P. 2008, Phys. Rev. D, 78, 043504
Zibin, J. P. 2011, Phys. Rev. D, 84, 123508